ISSN 2075-1087, Gyroscopy and Navigation, 2018, Vol. 9, No. 1, pp. 76–95. © Pleiades Publishing, Ltd., 2018.

Stochastic Error Modeling of Smartphone Inertial Sensors for Navigation in Varying Dynamic Conditions

Ahmed Radi*, Sameh Nassar, and Naser El-Sheimy

Department of Geomatics Engineering, University of Calgary, Calgary, AB T2N 1N4, Canada

**e-mail: ahmed.elboraee@ucalgary.ca*

Received October 28, 2017

Abstract—This paper aims at investigating and analyzing the behavior of Micro-Electromechanical Systems (MEMS) inertial sensors stochastic errors in both static and varying dynamic conditions using two MEMS-based Inertial Measurement Units (IMUs) of two different smartphones. The corresponding stochastic error processes were estimated using two different methods, the Allan Variance (AV) and the Generalized Method of Wavelets Moments (GMWM). The developed model parameters related to laboratory dynamic environment are compared to those obtained under static conditions. A contamination test was applied to all data sets to distinguish between clean and corrupted ones using a Confidence Interval (CI) investigation approach. A detailed analysis is presented to define the link between the error model parameters and the augmented dynamics of the tested smartphone platform. The paper proposes a new dynamically dependent integrated navigation algorithm which is capable of switching between different stochastic error parameters values according to the platform dynamics to eliminate dynamics-dependent effects. Finally, the performance of different stochastic models based on AV and GMWM were analyzed using simulated Inertial Navigation System (INS)/Global Positioning System (GPS) data with induced GPS signal outages through the new proposed dynamically dependent algorithm. The results showed that the obtained position accuracy is improved when using dynamic-dependent stochastic error models, through the adaptive integrated algorithm, instead of the commonly used static one, through the non-adaptive integrated one. The results also show that the stochastic error models from GMWM-based model structure offer better performance than those estimated from the AV-based model.

Keywords: Stochastic Error Modeling, Inertial Sensors Calibration, IMUs, Allan Variance (AV), Generalized Method of Wavelet Moments (GMWM), Dynamically Dependent Adaptive INS/GPS Algorithm

DOI: 10.1134/S2075108718010078

1. INTRODUCTION

The Global Navigation Satellite System (GNSS) is an accurate positioning system for different applications in outdoor environments. A major demerit of GNSS, is the performance degradation during GNSS signal outages [1]. On the other hand, the Inertial Navigation System (INS), classified as a dead-reckoning system, provides high frequency precise short-term navigation information. Nevertheless, a major drawback is related to the inertial sensors' errors that lead to accuracy degradation of navigation information with respect to time [2]. Over the last two decades, the integration of both systems provides an accurate, reliable and complementary system with better performance, in comparison to each stand-alone system. In GNSS/INS integrated systems, the GNSS provides the absolute positioning information while the INS is at the helm of attitude determination. However, some limitations regarding frequent occurrence of GNSS signal outages caused by signal blockages in some situations, such as tunnels and urban areas [3]. In these cases, the INS provide the navigation information, as a stand-alone system, until the GNSS signal are re-acquired. Therefore, the overall system positioning accuracy, during GNSS signal outages, is totally dependent on the quality of the INS sensor data which, in turn, could be improved if precise inertial sensor error models are implemented.

Recently, Micro-electro Mechanical Systems (MEMS)-based inertial sensors became an attractive candidate for INS/GNSS when compared to the traditional systems. Although MEMS-based inertial sensors have various advantages regarding cost and size reduction, low power consumption and light weight, some limitations concerning the overall accuracy should be addressed [4]. To be more specific, the fact that such cheap and small MEMS-based sensors rarely provide the required accuracy, in some applications, could not be denied [5]. The reason for that is related to additional unwanted error signals being added to the true value measured by the sensor and usually classified into two parts, deterministic and sto-

chastic [6]. The deterministic part such as sensor bias and scale factor, could be eliminated by laboratory calibration where sensor errors could be determined by comparing the sensor outputs with a known reference inputs [7], which are beyond the scope of this paper. On the other hand, stochastic errors require correct modelling and estimation using special noise characterization techniques. Consequently, both previously mentioned error types significantly influence the estimated position, velocity, and attitude which, in turn, reflects as a performance degradation of the overall navigational accuracy, especially when INS is working as a standalone system in areas of poor GNSS signals.

1.1. Review of Previous Work

Generally, inertial sensor stochastic modeling is considered to be a nontrivial and time-consuming task especially for low-cost MEMS-based sensors. This due to the complicated stochastic error model structure that may contain one or more random latent processes, e.g. White Noise (WN), correlated noise, Random Walk (RW), etc. Based on that, different stochastic modeling techniques have been used, some of them are time domain, others are frequency domain, to mitigate the inertial sensors error terms.

For instance, Autocorrelation function (ACF) technique was used in [8] and [9] to investigate the correlation time of consumer grade inertial sensor errors used for providing an attitude determination algorithm. However, according to be highly model-sensitive, correlation technique are not usually the best choice to deal with high dynamic range or higher order random processes [10]. Moreover, Power Spectral Density (PSD), which is the Fourier Transform (FT) of the ACF, has been used in some researches for inertial sensor error modeling [11, 12]. However, a major limitation of such technique is related to the low frequency part of the PSD log-log plot which still conveys some information but with quit high uncertainty. Such a drawback could highly affect the accuracy of identifying low frequency noise parameters while investigating long inertial sensor output noise datasets.

Moreover, an additional approach was presented in the mid-1960s, namely the multiple-model method [13]. Such an approach has been applied for structural and parametric identification of stochastic models, with their posterior probabilities computations utilizing a bank of Kalman filters (KF), where each individual KF is tuned for a specific model. Multiple-model method has been used in various fields including navigation and target tracking to solve different problems, for instance GPS ambiguity removal [14] and advanced tracking techniques that are based on decisions regarding target maneuvers [15]. However, constructing a set of KFs leads to dramatically increase the computational load which could be considered as a major demerit of such an approach, especially for real-time applications.

In addition to the above methods, the most widely used approach to study the stochastic characteristics of inertial errors is the Allan Variance (AV) which was basically introduced for studying the frequency stability of precision oscillators [16]. Due to being simple to compute, simple to understand and straightforward, AV has been used in numerous researches for identifying different types of random noise processes in inertial sensors measurement's [10, 17–20]. Nonetheless, applying AV to low-cost MEMS units revealed significant limitations. One of these limitations is regarding the ambiguity occurrence while representation a real AV log-log curve as a sum of two or more random processes.

A recently developed estimation method, called the Generalized Method of Wavelet Moments (GMWM) [21]. GMWM combine the Wavelet Variance (WV) and the Generalized Least Square (GLS) principle to finally estimate the so-called latent composite processes of a time series. Some recent research works used the GMWM to analyze simulated inertial sensor data [22] and actual data collected by various Inertial Measurement Units (IMUs) [23, 24]. Based on that, it is obvious how the AV and GMWM are based on the slope fitting techniques (KF-free techniques) which increase the potential of using both, even for future online estimation for noise parameters, to avoid computation complexity compared to the multi-model method.

However, almost all previous research work has a common limitation regarding investigating the environmental conditions effects on the stochastic error part for sensors under test. Specifically, it is known that the stochastic behavior of MEMS inertial sensor errors depends on the environmental conditions affecting the sensor such as temperature variation and platform dynamics. For instance, collecting long data sets using MEMS-based inertial sensor to construct AV curve usually increase the temperature of the silicon-based sensor (as silicon is the core material used for MEMS fabrication) under test which, in turn, affects the stochastic behavior of the residual error signals [25]. Based on that, stochastic error modeling based on long term data collected at room temperature cannot be accurate enough for MEMS-based units. In addition to the above, inertial sensors are being used to provide positioning and attitude in kinematic mode. In other words, these sensors are basically designed to work in dynamic environments. Thus, it is important, to investigate the relationship between inertial sensor error behavior and the vehicle dynamics which, in the same contest, means that the stochastic error modeling based on only static data will not guarantee the best accuracy.

Despite this awareness, few researchers investigated the behavior of MEMS inertial sensors stochas-

tic characteristics during different environmental conditions such as temperature variation [26, 27] and dynamics of the platform on which sensors are mounted [28, 29]. However, constructing and characterizing a dynamically dependent error processes for low-cost MEMS-based inertial sensors is an area that should be investigated more. Also, it is important to note that we previously examined the effect of the thermal variation on the noise model of different low-cost smartphone mounted MEMS-based IMUs in [30] using long test data sets. Due to investigating relatively short duration data sets in this article, the thermal variation effect could be neglected.

1.2. Aim and Scope of Study

The main objective of this paper is to improve the positioning accuracy of INS/GNSS integrated systems using dynamically dependent error models for low-cost MEMS IMUs used in smartphones. This main objective will be achieved through the following sub-objectives:

First, reveal the stochastic characteristics of MEMS inertial sensors and their changes due to dynamic conditions using reference signals provided in laboratory environment using an accurate single axis turn table. All navigation filters typically include residual deterministic sensor errors (e.g., gyro and accelerometer biases and scale factors) in the state vector. However, stochastic errors are commonly modelled by using relatively simple stochastic processes such as 1st order Gauss–Markov (GM), RW, and Random Constant (RC) processes. The stochastic parameters, which compose the navigation system error noise matrix in the used estimator, KF with feedback, are commonly set according to the RW in the datasheet. In this research, we performed abundant number of laboratory tests using two different IMUs, test results will be presented for both static and dynamic conditions as well. Also, we will also analyze whether we need to use more complex stochastic models for sensors work under various dynamic conditions, and choose different parameter settings according to the changes of platform dynamics.

Second, expose the link between the MEMS inertial sensor errors and platform dynamics using a suitable observation technique to investigate how the dynamics has an influence on the errors of the IMU under test. Two different methods, the most widely used AV and the recently proposed GMWM will be utilized. Thus, we would be able to investigate the advantages and limitations of the AV method in identifying low-cost MEMS sensor error sources and computing the error parameters quantification under various laboratory dynamic conditions.

Third, propose a new dynamically dependent integrated navigation algorithm, which is an extension to what was introduced in [31]. Such an algorithm uses an additional adaptive function to automatically switch between different stochastic error parameters values according to the applied platform dynamics to finally eliminate dynamics-dependent effects. The general layout of the proposed adaptive algorithm will be given.

Finally, evaluate the performance of estimated model parameters based on both aforementioned approaches using the proposed adaptive loosely coupled INS/GPS integration architecture and during GPS signal outage periods, i.e., the navigation states are determined independently from GPS data. We will clarify how obtained stochastic sensor models associated with the proposed dynamically dependent navigation algorithm lead to more robust navigation solution based on low-cost MEMS units.

2. METHODOLOGY

2.1. Inertial Sensor Errors' Stochastic Processes

Generally, inertial sensors' measurements have various errors which contaminate the true measurements from the gyroscopes and the accelerometers. Therefore, in order to obtain an optimal navigation solution, the first step starts with evaluating the deterministic sensor errors such as bias and scale factor. Such deterministic errors could be eliminated by proper laboratory calibration of the inertial measurement unit sensors [32]. Another type of errors has random nature and known as stochastic sensor errors. The impact of deterministic and stochastic sensor errors can be mitigated through deterministic and stochastic modelling, respectively.

The main random processes related to inertial sensors are briefly defined as follow:

• *Quantized Noise (QN)*: The small difference between the real amplitude of the point under sampling and the bit resolution of the Analog-to-Digital Converter (ADC) is called a quantization error [33].

• *White Noise (WN)*: The random amount added to the actual signal and with a long term average equals to zero is defined as white noise [34]. This noise term is often known as Angular/Velocity Random Walk (ARW/VRW) for gyros and accelerometers, respectively.

• *Bias Instability (BI)*: Also known as flicker noise and generally this type of noise is related to the instability of the bias offset for a sensor output measured in ideal environment [34].

• *Random Walk (RW)*: As defined in [35] and [10], RW is a random process of uncertain origin, possibly known as a very low frequency noise term. Mathematically, RW is an integral to the WN.

This noise term is often known as Rate/Acceleration Random Walk (RRW/AccRW) for gyros and accelerometers, respectively.

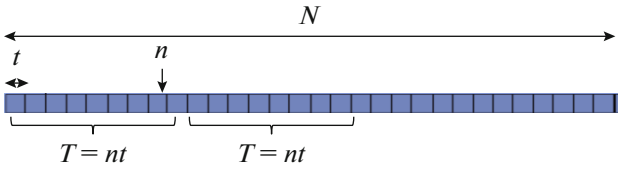

Fig. 1. Allan variance (AV) data structure.

• *Drift Ramp (DR)*: A very low frequency noise process that is often called Drift Rate/Acceleration Ramp (DRR/DAccR) for gyros and accelerometers, respectively.

• *Gauss Markov (GM)*: If a Gaussian process has an exponentially correlation time, it is called a Gauss-Markov (GM) process as defined in [6]. Generally, GM process can have any order. However, in this paper we are only interested in the stationary 1st order one. Sometimes it is used as an approximation for the BI noise term [36].

2.2. Allan Variance

Allan Variance (AV) is a method of representing the Root-Mean-Square (RMS) random drift error as a function of averaging times [16]. Originally, it was developed to study the frequency stability in clocks, oscillators and amplifiers in the mid-1960s by David Allan. Later, it was used to identify different latent random processes hidden in different measurements [17].

Moreover, AV is known to be simple to compute, much better than having a single RMS drift number to apply to a system error analysis, and also simple to understand [10].

The calculation process for the standard AV could be illustrated as follow [37]:

• Divide the whole dataset into smaller number of clusters, each with a cluster length (T) as illustrated in Fig. 1.

• Calculate the mean value of each cluster individually.

• Calculate the difference between the mean values of every two consecutive clusters.

• Calculate the mean square of these differences and divide by a certain factor. This value is called the AV (σ^2) related to the cluster time (T).

• Change the cluster time (T) from small value to a larger one and recalculate the AVs, thus we can represent the signal instability on different time scales.

• Draw the AV plot which is a log–log plot of the AV versus the cluster time (T) in order to analyse the error characteristics.

Consequently, the mathematic form of the AV is:

$$\sigma^2(T) = \frac{1}{2(N-2n)} \sum_{k=1}^{N-2n} \left[\bar{\Omega}_{\text{next}}(T) - \bar{\Omega}_k(T)\right]^2, \quad (1)$$

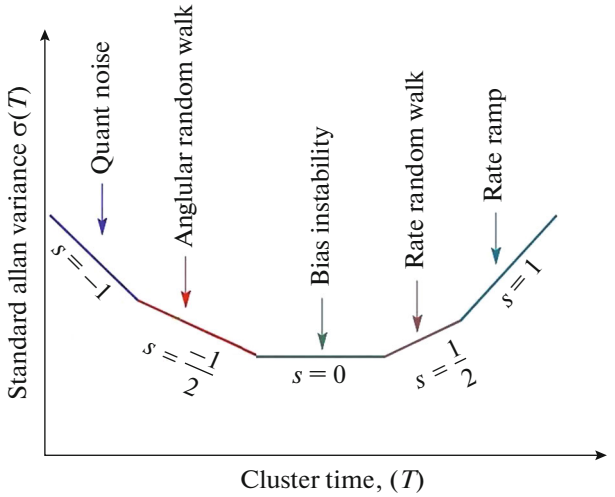

Fig. 2. Noise segments identification on Allan deviation plot (after [27]).

where $\bar{\Omega}_k(T)$ is the mean value of the k cluster, the term $\bar{\Omega}_{\text{next}}(T) - \bar{\Omega}_k(T)$ stands for the average operation for each of two adjacent clusters as next $= k+1$, N is the total number of data points for the entire run and $n+1$ is the number of data points in each cluster, satisfying $(n < N/2)$.

Since the AV is being used to analyze the sensor output measurements, then there should exist a relationship between the AV and the Power Spectral Density (PSD) of the latent random process hidden in the aforementioned measurements. Such a relationship was illustrated by [10] as follow:

$$\sigma^2(T) = 4\int_0^\infty S_\Omega(f) \frac{\sin^4(\pi f T)}{(\pi f T)^2} df, \quad (2)$$

where $S_\Omega(f)$ is the PSD of the stochastic process $\Omega(T)$ and the term $\sin^4(\pi f T)/(\pi f T)^2$ is the transfer function of the applied filter.

Different types of stochastic processes of particular interest for inertial sensors, which are either known to exist in inertial sensors or are suspected to influence the inertial data, are illustrated in Fig. 2 (QN, ARW/VRW, BI, RRW/AccRW, DRR/DAccR) and 1st order GM process), as well as the corresponding slopes of the standard deviation obtained from the Allan deviation plot where the figure highlights the theoretical Allan deviation log-log plot.

It is clear that AV works successfully because different noise terms operate in different frequencies. In this paper, the characteristic curve is first obtained by applying the AV algorithm to the entire data. The curve is then measured to determine the types and magnitudes of certain random errors possibly residing in the data according to its slope. Finally, the random

errors are identified and modelled. This operation is being carried out within laboratory environment for static data, and then repeated for various dynamic conditions through a single axis turn table. Detailed AV mathematical calculation steps can be found in [38] and [37].

2.3. Generalized Method of Wavelet Moments

GMWM is an estimation method based on the idea of Generalized Method of Moments (GMM) estimators [39] which is based on using the Wavelet Variance (WV), defined as the variance of a process after it has been subject to an approximate bandpass filter . The GMWM makes use of the relation between the WV and the parameters of a latent process, estimating the latter by minimizing the distance between the empirical and model-based WV [21]. The calculation process for the GMWM can be illustrated as follow:

• Applying a wavelet filter $h_{j,l}$, where $j = 1,\ldots,J$ is the wavelet filter level of length $L_j = \left(2^j - 1\right)(L_1 - 1) + 1$, Haar wavelet filter in this paper, to the stationary or non-stationary process Y_t, we get the Maximum Overlap Discrete Wavelet Transform (MODWT) coefficients $W_{j,t}$

$$W_{j,t} = \sum_{l=0}^{L_j - 1} h_{j,l} Y_{t-l}, t \in \mathbb{Z}. \quad (3)$$

• Using the previous equation, the WV could be defined as the variance of the wavelet coefficients

$$\nu_j = \mathrm{var}\left(W_{j,t}\right) \quad (4)$$

• For a finite observed processes, the MODWT estimated WV can be calculated as follow [40]:

$$\hat{\nu}_j = \frac{1}{M_j} \sum_{t=L_j}^{N} W_{j,t}^2, \quad (5)$$

where: $M_j = N - L_j + 1$ is the total number of wavelet coefficients at the considered time scale.

• A direct relationship between the WV and PSD exists where the variance of the mentioned series of wavelet coefficients is the direct integral of its PSD as follow [41]:

$$\nu_j(\theta) = \int_{-1/2}^{1/2} S_{W_j}(f)\, df = \int_{-1/2}^{1/2} \left|H_j(f)\right|^2 S_{F_\theta}(f)\, df, \quad (6)$$

where $H_j(f)$ is the transfer function of the filter $h_{j,l}$, F_θ is the model built using one or more stochastic processes that describe the dynamics of the observed sensor error sequence and S_{F_θ} is the PSD implied by the model F_θ.

• The GMWM estimator is being used to minimize the distance between the empirical and estimated WV in order to estimate the parameters of the latent composite processes as follow [23]:

$$\hat{\theta} = \underset{\theta \in \Theta}{\mathrm{argmin}} \left(\hat{\nu} - \nu(\theta)\right)^T \Omega \left(\hat{\nu} - \nu(\theta)\right), \quad (7)$$

where θ represents the time series model parameter vector that we intend to estimate belonging to the compact set Θ and Ω is a symmetric positive definite weighting matrix chosen in a suitable manner to make the GMWM estimator is as efficient as possible [42]. It is also important to mention that this method could also be based on the AV since the aforementioned Haar WV is simply twice the AV with additional benefits [43, 44]. A full theoretical flowchart for the GMWM calculation steps is illustrated in Fig. 3 [30].

The standard WV is being calculated to obtain the characteristic curve. Robust WV is also computed, compared to the standard calculated WV to check the existence of any outliers in the data. The next step is the estimation of the model parameters where more than one model can be estimated and ranked using the Wavelet Information Criteria (WIC), which will be discussed in Section 3.4, to determine which model is the best. Detailed mathematical background for the GMWM can be found in [21] and [45].

3. EXPERIMENTS AND ANALYSIS FOR STATIC/DYNAMIC DATA USING AV AND GMWM

Tests were conducted to identify the major noise terms existing in the smartphone mounted MEMS units. Since we focus more on the stochastic performance of gyros in this paper, the data were collected at the University of Calgary (UofC) using the Animatics SmartMotor™ Series 4 Single-Axis Positioning and Rate Table (Fig. 4). The table has a rate accuracy of 0.02% (Over 1 revolution) and was pre-levelled before starting data collection. Also, based on previous experiences regarding the locations of internal inertial modules through smartphone disassembling [46], each smartphone was fixed on the turntable where the sensitive axes of both the Z-gyro and the turntable are aligned, as much as possible, to ensure acceptable measurement accuracy. The data was collected in two different modes, the first one is the static mode and the second is the dynamic mode. Static data sets were collected first at room temperature using MEMS-based IMUs inside two different smartphones, namely Samsung Galaxy S4 and Apple iPhone 5S. For the IMUs inside the tested smartphones, the Apple iPhone 5S is equipped with a 3D accelerometer (Bosch Sensortec BMA220, Gerlingen, Germany) and an integrated 3D gyroscope (ST-Microelectronics, L3G4200DH, Geneva, Switzerland). On the other hand, the Samsung Galaxy S4 has an InvenSense MPU-6500 inertial module which is a 6-axis motion

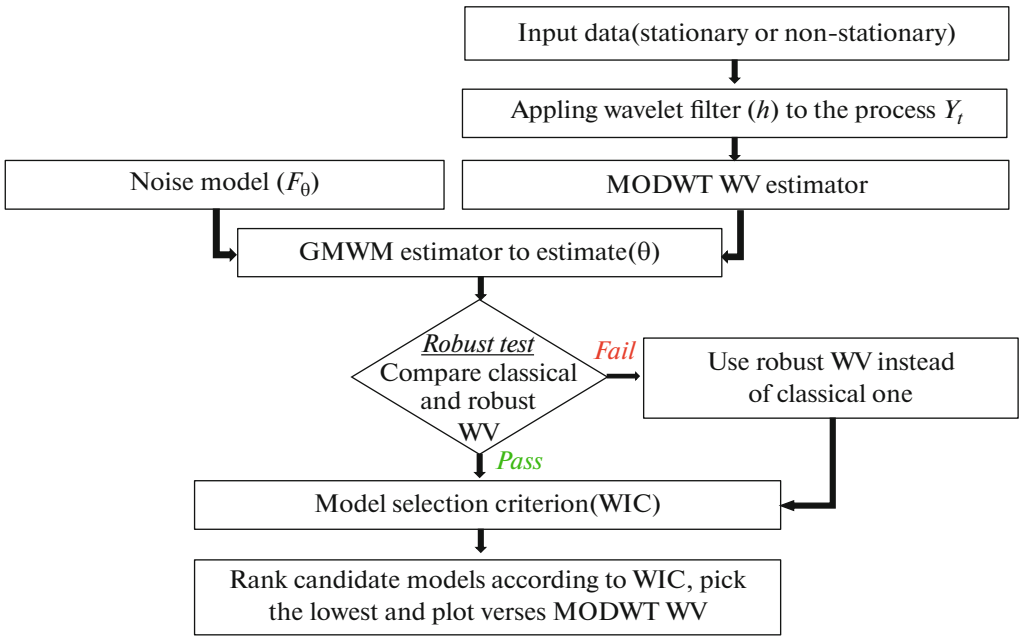

Fig. 3. GMWM estimator flowchart [30].

tracking device that combines a 3-axis gyroscope, 3-axis accelerometer, and a Digital Motion Processor (DMP) all in a small 3 × 3 × 0.9 mm package.

3.1. Static Data

The IMU static data was sampled at 20 Hz and 100 Hz for the Samsung Galaxy S4 and Apple iPhone 5S respectively for about 15 minutes at room temperature. The reason for choosing such data length will be discussed later.

The performance of each inertial sensor of the two MEMS-based IMUs is estimated using AV and GMWM to study the noise characteristics and identify the corresponding sensor stochastic error model parameters. This was performed for the two different modes, static and dynamic. Fig. 5 shows the AV plot for the Samsung Galaxy S4 and Apple iPhone 5S Z-Gyro measurements (static mode) while Table 1 lists the corresponding identified error coefficients after AV analysis for the Z-Gyros. According to having identical sensors at the same inertial module, we provided the analysis of one gyro, Z-Gyro, for each module to avoid redundant results.

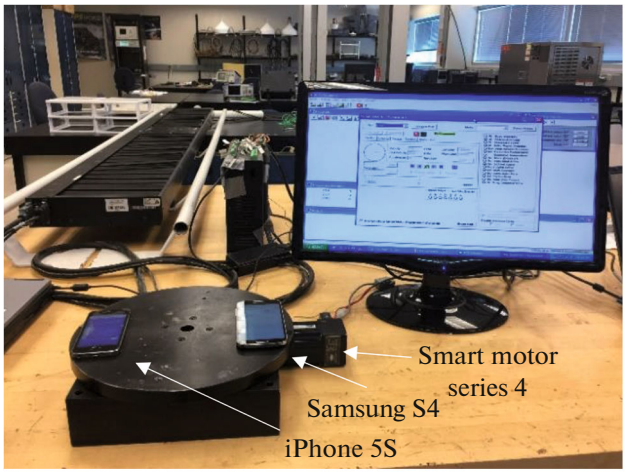

Fig. 4. Animatics SmartMotor™ Series 4 single axis positioning and rate Table.

From Table 1 and using slope fitting, it is clear that the ARW is the dominant noise parameter that could be observed for both Samsung Galaxy S4 and Apple iPhone 5S gyros as it is considered to be the high frequency noise term that appears at slope −1/2. Other low frequency noise terms such as correlated noise require long-term data in order to be observable.

3.2. Dynamic Data

After performing the AV analysis on the static data, additional analysis is needed to see how the inertial sensor noise parameters change with dynamics. Different quantities could be used to define the meaning of "dynamics". Such quantities could be summarized as linear velocity (v), linear acceleration $(\dot{v})$, linear jerk $(\ddot{v})$, angular velocity (ω), angular acceleration $(\dot{\omega})$ and angular jerk $(\ddot{\omega})$ [47]. In this paper, we are interested in investigating the effect of angular velocity (ω) and angular acceleration $(\dot{\omega})$ on stochastic model parameters of MEMS inertial sensors mounted on the

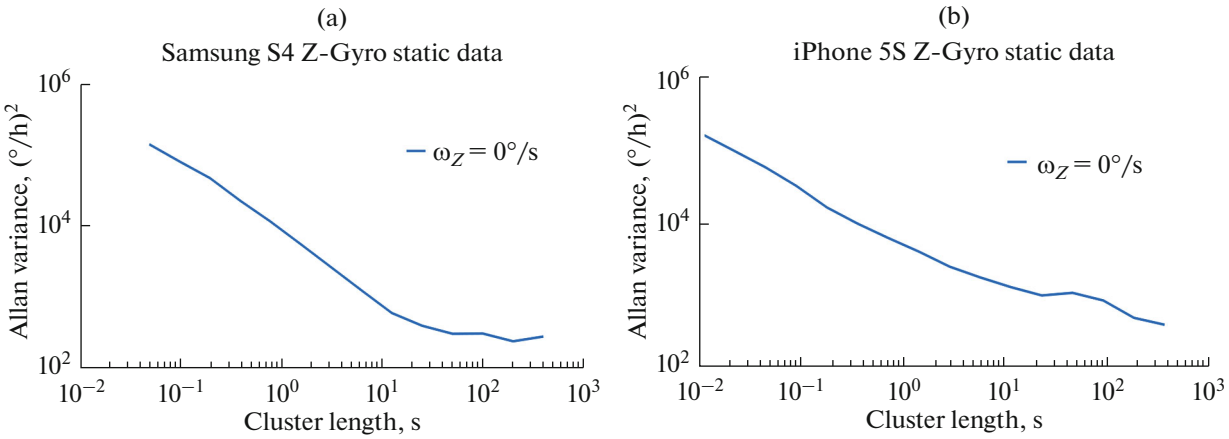

Fig. 5. Allan variance log-log plot for smartphone gyro measurements at static mode (a) Samsung Galaxy S4 Z-Gyro (b) Apple iPhone 5S Z-Gyro.

aforementioned smartphones. Using the Animatics SmartMotor™ Series 4 Single-Axis Positioning and Rate Table commands, it is possible to let the turntable rotate with, for example, a constant angular velocity (defined as reference signal) and collect inertial measurements from the smartphones fixed on the turntable (defined as measured signal).

The sensor error signal (defined as residual signal) is simply the difference between the measured signal and the reference one. The next step will be to study the relation between residual signal and the applied platform dynamics. As mentioned for static data collection, dynamic data was collected at the same previously mentioned sampling rates as well as room temperature.

3.2.1. Constant Angular Velocity and Angular Acceleration

In order to study the effect of the applied angular velocity and angular acceleration, different angular velocity and acceleration commands were sent to the Animatics SmartMotor™ turntable via SmartMotor Terminal Window. First, such commands allow the turn table to rotate with five constant (fixed) angular velocities that represent the mentioned reference signal for 15 minutes. The angular velocity values are (9, 18, 36, 72 and 120 deg/s; respectively). Thus, the performed test covers the ordinary operational angular velocity of smartphones. Second, starting from initial angular velocity equals to zero ($\omega_{z_0} = 0$) and making use of the Animatics SmartMotor™ turntable, different angular acceleration values were applied, specifically 1 and 2 deg/s^2. It is important to mention that both static and dynamic data (used for angular velocity investigation) have equal data length and collected at the same lab. Thus, the only factor to be changed is the applied dynamic quantity. Consequently, fair judgment could be obtained. At each angular velocity/acceleration value, the data was collected twice for both smartphones. The main reason for this is to make sure that the performance of each sensor is almost the same when repeating the same test, i.e. to ensure the repeatability factor for the tested inertial sensors.

In additional to that, one major common concern of most of the inertial sensors calibration techniques is the time synchronization between the IMU output measurements and the reference signal. Since the IMU under test and the turntable, considered as a source of reference signal, are two separate (self-contained) systems, the clock difference might cause data alignment discrepancies during the signal comparison process [48]. To avoid that, the first and last 30s of each dataset collected at each applied angular velocity were discarded. The reason for that is to dodge the regions at which the turntable is accelerating or decelerating and to ensure constant applied angular velocity as well.

For angular acceleration experiments, data length will be shorter than angular velocity measurement. The main reason for this is that the Animatics SmartMotor™ turntable used for reference signal has a maximum angular velocity "threshold" that could not be run over. Such a limit allows the collection of data with

Table 1. Identified error coefficients after AV analysis for Samsung Galaxy S4 and Apple iPhone 5S Z-Gyros (static mode)

Exp. no.	Noise coefficient	ARW "N" deg/$\sqrt{\text{h}}$
Samsung S4 Z-Gyro		
0	$\omega_z = 0°/\text{s}$	1.5511
Apple iPhone 5S Z-Gyro		
0	$\omega_z = 0°/\text{s}$	1.0978

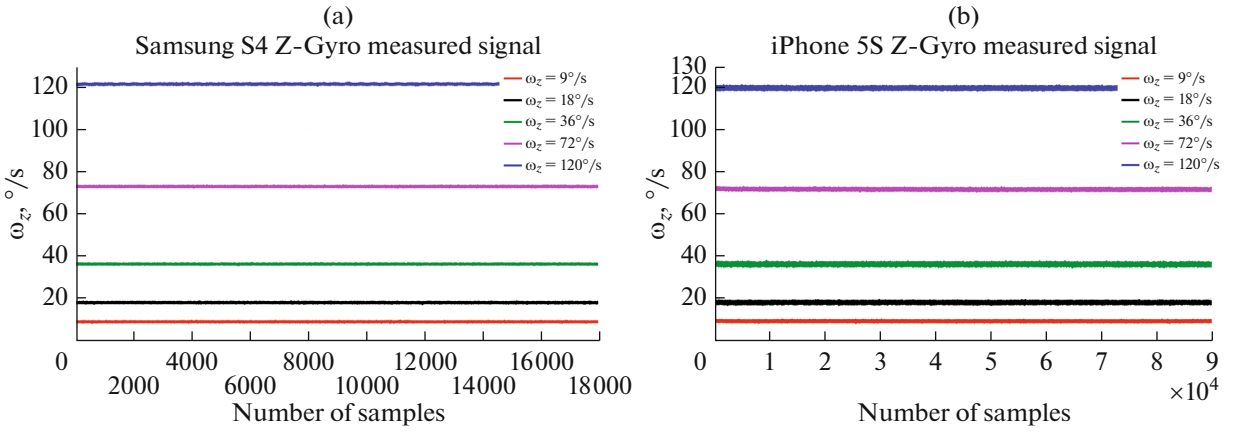

Fig. 6. Measured signals for smartphone gyro measurements (applied different angular velocities for 15 minutes) (a) Samsung Galaxy S4 Z-Gyro (b) Apple iPhone 5S Z-Gyro.

length 225 and 155 s for $\dot{\omega}$ equals to 1 and 2 deg/s^2; respectively. Moreover, attention was paid to consider gyro measurements starting just after zero till 225 and 155 deg/s for applied angular acceleration of 1 and 2 deg/s^2, respectively, to ensure synchronized measurements.

Figure 6 shows the signal measured by the Z-gyro for Samsung Galaxy S4 and Apple iPhone 5S after applying different angular velocity (ω_z) using the turntable. In general, Fig. 6 display that the Apple iPhone 5S gyro has higher noise level than the Samsung Galaxy S4 one. Moreover, it is visually noticeable how that the Apple iPhone 5S gyro has different levels of noise at different applied angular velocities, while this is not so visible in case of the Samsung Galaxy S4 gyro.

Each data set was collected under fixed value of angular velocity/acceleration, the reason for that is referred to the tools used for the data analysis, i.e. AV and GMWM. To be more specific, these tools require situational environment for the stochastic behaviour [28] which could be obtained under fixed values of dynamic quantity for each experiment, for instance fixed angular velocity/acceleration. Also, Figure 7 highlights the signal measured by the Z-gyro for Samsung Galaxy S4 after applying angular acceleration $(\dot{\omega}_z)$ using the turntable. Fig. 7 illustrates both sensor measured signal and reference signal designated in blue and red colors, respectively.

It is clear how the gyro output (measured angular velocity) forms a triangular or trapezoidal motion profile due to the applied ascending angular acceleration.

To get the residual signal in each experiment, the reference signal value is being subtracted from the measured Z-gyro signal illustrated in Fig. 6 and Fig. 7. Figure 8 gives an example of the residual signal for the Samsung Galaxy S4 Z-Gyro measurements after applying 9 deg/s constant angular velocity.

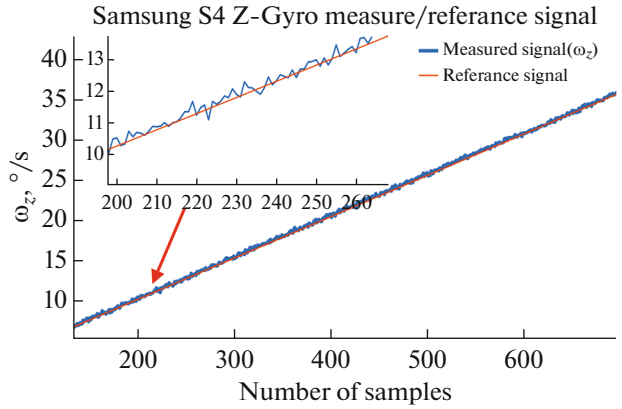

Fig. 7. Measured signal for Samsung Galaxy S4 Z-Gyro (applied angular acceleration for 225 s).

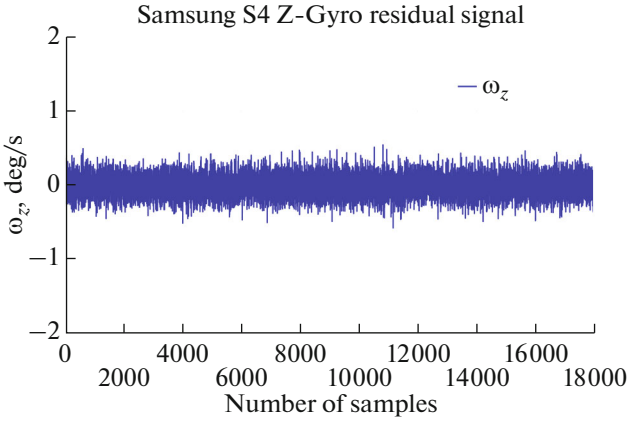

Fig. 8. Residual signal for Samsung Galaxy S4 Z-Gyro measurements (dynamic mode with applied 9 deg/s).

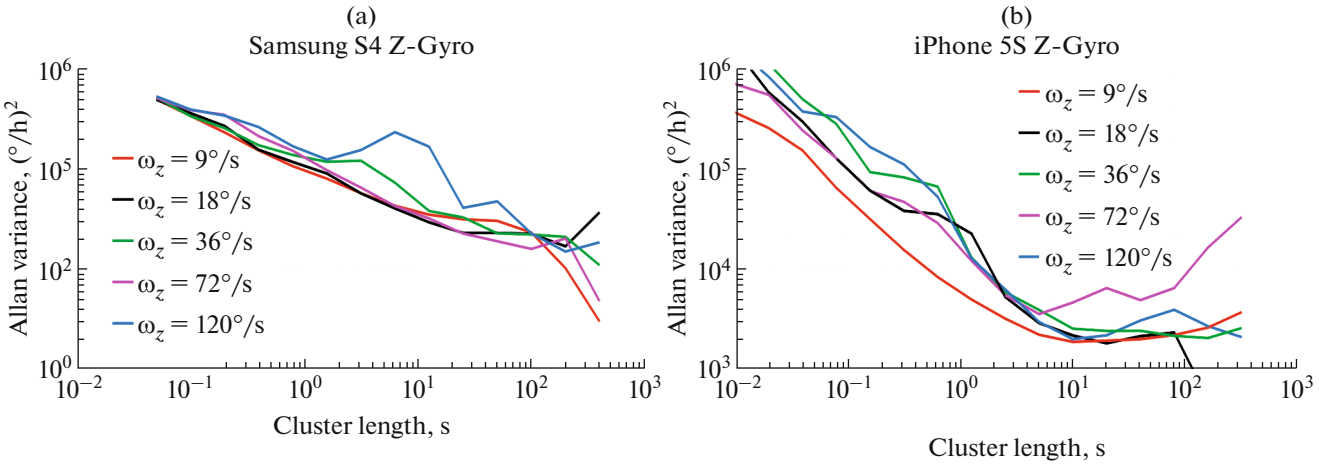

Fig. 9. Allan variance log-log plot for smartphone gyro measurements at dynamic mode (a) Samsung Galaxy S4 Z-Gyros (b) Apple iPhone 5S Z-Gyros.

3.3. Allan Variance Analysis

Figure 9 shows the AV for Samsung Galaxy S4 and Apple iPhone 5S Z-Gyro measurements while Table 2 lists the identified error coefficients after AV analysis for Z-Gyros.

Table 2 shows the direct effect of changing dynamics on the estimated stochastic error model parameters' values. Such an effect leads to the importance of having a dynamic dependence stochastic model for the aforementioned sensors. Regarding the 15 minutes data sets, the practical reason for choosing it is that in many applications, the major concern is usually only for the short-term performance while in long-term the INS errors can be corrected by integrating the IMU with other systems, e.g. GPS through a KF. For such data sets, which are considered to be "short" data, it is clear that the ARW is the dominant noise parameter that could be observed which is similar to the AV analysis performed for static data sets.

Other noise parameters such as correlated noise and drift ramp need large amount of data in order to be observable [49]. Consequently, Table 2 clarifies how the ARW is the dominant noise term for short cluster lengths. However, increasing the angular velocity value always affects ARW values for both Samsung Galaxy S4 and Apple iPhone 5S gyros. Specifically, the change of the Samsung Galaxy S4 ARW parameter reached more than 62% with angular velocity changes from static condition to 120 deg/s. Moreover, the change of the Apple iPhone 5S gyro ARW parameter is more obvious where it reached about 128% for the same range of angular velocity change. This analysis illustrates how the ARW parameter related to the Apple iPhone 5S gyro is more sensitive to the measured angular velocity value than the Samsung Galaxy S4 one. Other stochastic noise parameters, such as BI, could hardly be detected.

Table 2. Identified error coefficients after AV analysis for Samsung Galaxy S4 and Apple iPhone 5S Z-Gyro measurements (dynamic mode)

Exp. no	Noise coefficient	ARW "N" $\mathrm{deg}/\sqrt{\mathrm{h}}$	BI "B" deg/h	RRW "K" $\mathrm{deg}/\mathrm{h}^{3/2}$
Samsung S4 Z-Gyro				
1	$\omega_z = 9°/\mathrm{s}$	1.6087 (I)	...	...
2	$\omega_z = 18°/\mathrm{s}$	1.7695 (I)	33.2482	...
3	$\omega_z = 36°/\mathrm{s}$	1.8353 (I)	...	...
4	$\omega_z = 72°/\mathrm{s}$	2.0574 (I)	23.8295	...
5	$\omega_z = 120°/\mathrm{s}$	2.5242 (I)	...	...
6	$\dot{\omega}_z = 1°/\mathrm{s}^2$	2.5656 (I)	...	...
7	$\dot{\omega}_z = 2°/\mathrm{s}^2$	2.4189 (D)	...	...
Apple iPhone 5S Z-Gyro				
1	$\omega_z = 9°/\mathrm{s}$	1.1788 (I)	66.3658	...
2	$\omega_z = 18°/\mathrm{s}$	1.702 (I)	...	...
3	$\omega_z = 36°/\mathrm{s}$	2.4233 (I)	...	...
4	$\omega_z = 72°/\mathrm{s}$	1.6711	90.1593	17.2218
5	$\omega_z = 120°/\mathrm{s}$	2.5048 (I)	68.5729	...
6	$\dot{\omega}_z = 1°/\mathrm{s}^2$	3.4811 (I)	...	...
7	$\dot{\omega}_z = 2°/\mathrm{s}^2$	3.0855 (D)	...	...

(I) Increased, (D) decreased.

Regarding the angular acceleration, only an ARW noise term could be detected for both Samsung Galaxy S4 and Apple iPhone 5S gyros. The reason for that is having a short data length due to the previously mentioned limitation of the turntable usage. Results from Experiments 6 and 7 shows that applying angular acceleration always increases the ARW value of the gyro under test for both smartphones when compared to static data (Experiment 0). For more numerical details, the ARW value growth is 65 and 56% for the Samsung Galaxy S4 Z-Gyro and 217 and 181% for the Apple iPhone 5S. It is clear that the angular acceleration effect on the white noise value is larger than the angular velocity effect on the same stochastic parameter even for a shorter time. Though, increasing the angular acceleration value showed a reversal effect on the Samsung Galaxy S4/Apple iPhone 5S gyros compared to increasing the angular velocity.

In addition, Table 2 shows how the change of the ARW parameter for the Samsung Galaxy S4 Z-Gyro reduced by almost 6% with angular acceleration changes from 1 to 2 deg/s^2. Taking into consideration that we only used two sets of data for such analysis, this could be considered a low percentage compared to the angular velocity effect.

In addition to that, similar behaviour was detected for the Apple iPhone 5S Z-Gyro where the change of its ARW parameter is slightly more obvious as it decreased to 13% of its value for the same range of angular acceleration increase. However, using short data with only two angular acceleration values might be the reason for having a contradiction between angular velocity and angular acceleration effects, with respect to the ARW behaviour. Consequently, longer data is highly recommended with more angular acceleration values in order to fairly judge the angular acceleration effect on ARW noise parameter. Also, longer data could allow low frequency noise parameters, for instance correlated noise and DRR, to appear.

3.4. Generalized Method of Wavelet Moments Analysis

The GMWM was proposed lately by some researchers to estimate the so-called latent or composite process. In order to attain an accurate noise model for any measured signal using the AV approach, it should be guaranteed that the data under test is "clean", i.e. free of contaminations, outliers or any extreme observations that might be hidden inside the data. In general, this is not an easy task to accomplish. On the other hand, the GMWM offers a way to overcome such issue by simply replacing the estimated WV with the robust M-estimator proposed by [43]. This estimator has well-defined asymptotic properties as well as better finite sample performance compared to other existing estimators. To be more specific, the WV estimator illustrated in Equation (5) is not robust and can be considered to be biased in the presence of outliers or different forms of contamination. In order to obtain a WV estimator that can be robust, Equation (5) should be re-expressed as an M-estimator $(\bar{v}_j)$ which is based on having stationary and ergodic wavelet coefficients, $\bar{W}_{j,t}$. A signal is known to be ergodic if its statistical properties could be identified from a single, sufficiently long and random sample of the process. When comparing both the robust and the classical WV to do such a contamination test, if there is significant difference over the initial time scales such as one WV lying outside of the other's 95% Confidence Interval (CI), then it is generally better to use the robust version as this means that the contamination test fails. Otherwise, the classical WV would be appropriate for such data with an indication of having an outliers' free data set [22]. As a next step, the top part of Fig. 10 shows how the contamination test was applied on Samsung Galaxy S4 Z-gyro residual signal obtained from rotating the Animatics SmartMotor™ turn table with an angular velocity value of 9 deg/s. It is obvious that both classical and robust WVs are lying inside each other's CI, noticing that the light-brown area is the overlapping between both classical and robust CI's. Consequently, such data is considered to be "clean", i.e. contamination free, which means that we can use the classical WV for model parameters estimation.

On the other hand, the right hand-side of Fig. 10 shows how the contamination test fails with Experiment 4 (where 72 deg/s angular velocity was applied) for Apple iPhone 5S Z-Gyro data set. This could be designated by the red circle area where the robust WV lies outside the CI of the classical one. Considering the fact that the Apple iPhone 5S data set for Experiment 4 contains outliers, and referring to Table 2, it is noticeable that the ARW value of this specific data set does not follow the general pattern as the other data sets. Moreover, the appearance of RRW noise parameter only in this data set is another clue that confirms the idea of how such data is contaminated. Therefore, we will not depend on the AV analysis for the data collected using the Apple iPhone 5S for Experiment 4. After the contamination test, it is important to identify the most accurate noise model for each data set individually. Based on the length of data sets, a set of nine candidate models were constructed for the Samsung Galaxy S4 and Apple iPhone 5S Z-gyros at each data set just to demonstrate the concept of modelling selection. Candidate models are illustrated in Table 3 with their related model parameters.

The main outcome of model selection process is to find the model that describes the latent stochastic processes of the inertial sensor data sets under test [44]. Usually, more than one model, among a list of candidate models, could describe such behaviour. To ensure maximum accuracy, GWMW provides the ability to select the best model based on WIC which illustrates in general how well the estimated model can predict

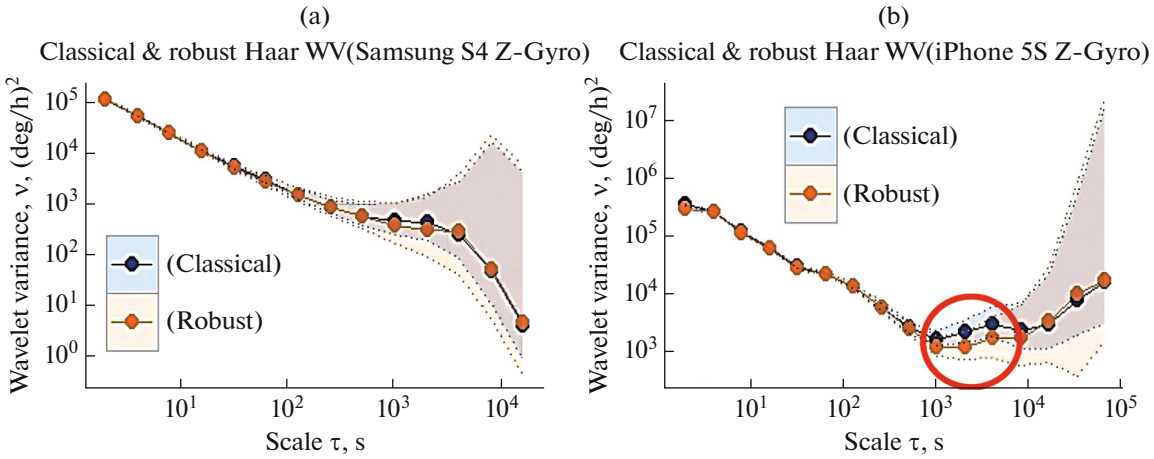

Fig. 10. Comparison between classical and robust WV for Samsung Galaxy S4 Z-Gyro and Apple iPhone 5S Z-Gyro (dynamic mode with applied 9 and 72 deg/s).

the values of the WV issued from another realization of the same process [23].

Mathematically, such criterion could be highlighted as follow:

$$\mathrm{WIC} = \underbrace{\left(\hat{v} - v\left(\hat{\theta}\right)\right)^{T} \Omega \left(\hat{v} - v\left(\hat{\theta}\right)\right)}_{\text{Objective Function}} + \underbrace{2\mathrm{tr}\left(\mathrm{cov}\left[\hat{v}, v\left(\hat{\theta}\right)\right]\Omega\right)}_{\text{Optimism}}. \quad (8)$$

The above-mentioned criterion is based on two terms. The first one is called the "Objective Function" which is related to the goodness-of-fit of each candidate model. This term usually decreases as the number of model parameters is increased to reach a better fitting with the observed signal WV. The second term is called the "Optimism" which represents the complexity of the model. Consequently, its value increases with increasing the number of model parameters as a penalty for over fitting. The sum of both terms gives the WIC which could be considered as a way to judge how adequate the selected stochastic model is suitable for the data under test [23]. It is important to mention that $v(\hat{\theta})$ values are being calculated by given a number of observations and a hypothetical model F_{θ}. However, a possible extension of the GMWM where analytical expression for $v(\hat{\theta})$ exists was proven to be too complicated [21]. By calculating the WIC for each model listed in Table 2, the model ranking operation was performed and the best model would be the one with the smallest WIC value, which was model 1 and 6 for the Samsung Galaxy S4 and the Apple iPhone 5S Z-gyros, respectively.

Table 3. Candidate models for Samsung Galaxy S4 and Apple iPhone 5S Z-Gyro measurements

Model number	Candidate models
Model # 1	WN
Model # 2	WN + GM
Model # 3	WN + GM + RW
Model # 4	WN + GM + DR
Model # 5	WN + GM + RW + DR
Model # 6	WN + 2*GM
Model # 7	WN + 2*GM + RW
Model # 8	WN + 2*GM + DR
Model # 9	WN + 2*GM + RW + DR

Based on the proposed criteria, the estimated parameters of the error models are calculated for the Samsung Galaxy S4 Z-Gyro and Apple iPhone 5S Z-Gyro under different angular velocity/acceleration values. Figure 11 shows the comparison between empirical and implied (estimated) WVs for the two aforementioned gyros at some selected values of ω_z. Equivalent results are highlighted in Table 4 which shows the influence of dynamics changing on the model parameters for both Z-Gyro.

For both Z-gyros, Table 4 highlights how the gyro noise model structure did not change due to changing a certain applied dynamics value. To be more specific, a model composed of only white noise was detected to be the best fit model for all values of angular velocities/acceleration related to the Samsung Galaxy S4 Z-Gyro. Also, for angular velocity effect, a white noise random process added to two 1st order GM processes was selected for all error measurement related to the Apple iPhone 5S Z-Gyro.

The direct effect of changing the applied dynamics was reflected in the magnitude of the aforementioned noise parameters. Compared to the static data results, increasing the angular velocity value mostly affects the ARW value to be increased for both Samsung Galaxy

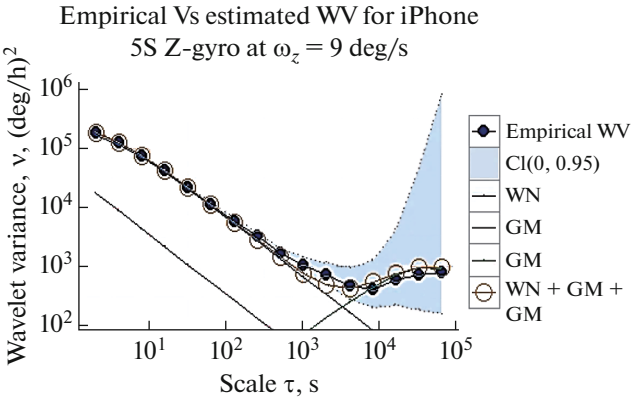

Fig. 11. Comparison between empirical and estimated WV based on model #6 (WN+2GM) for Apple iPhone 5S Z-Gyro (dynamic mode with applied 9 deg/s).

S4 and Apple iPhone 5S gyros with a maximum increasing percentage of 41 and 986%; respectively. Such behaviour was repeated in the case of angular acceleration increase as well. In addition, the ARW values increase to 55 and 51% for the Samsung Galaxy S4 Z-Gyro and to 409 and 165% for the Apple iPhone 5S Z-Gyro; respectively.

Regarding correlated noise processes, a combination of two 1st order GM processes could be observed under all angular velocity points but with different response according to applied angular velocity value. Specifically, according to the Samsung Galaxy S4 Z-Gyro, both variances of the GM1 (σ^2_{GM1}) and GM2 (σ^2_{GM2}) mostly increase with raising the angular velocity with a maximum change reached over 161% for σ^2_{GM1} and approximately 19% for σ^2_{GM2}. On the other hand, (β_1), which is the reciprocal of the correlation time, appears to have reversal behaviour as it first increases and then decreases with a maximum degradation percentage of 90%. Unfortunately, the pattern of β_2 could not be well-detected with dynamics and angular velocity variation. Due to shorter data sets for angular acceleration experiments, only one 1st order

Table 4. Identified Error Coefficients after GMWM Analysis for Samsung Galaxy S4 Z-Gyro and Apple iPhone 5S Z-Gyro Measurements based on Model # 1 (WN) and 6 (WN + 2GM), Respectively

Exp. no	Noise coefficient	WN(ARW) "*N*" $\mathrm{deg}/\sqrt{\mathrm{h}}$	GM1 β_1, σ^2_{GM1} $1/\mathrm{s}, (\mathrm{deg}/\mathrm{h})^2$	GM2 β_2, σ^2_{GM2} $1/\mathrm{s}, (\mathrm{deg}/\mathrm{h})^2$
Samsung S4 Z-Gyro				
0	$\omega_z = 0°/\mathrm{s}$	2.5342	...	...
1	$\omega_z = 9°/\mathrm{s}$	2.7865 (I)	...	...
2	$\omega_z = 18°/\mathrm{s}$	2.8379 (I)	...	...
3	$\omega_z = 36°/\mathrm{s}$	2.8653 (I)	...	...
4	$\omega_z = 72°/\mathrm{s}$	2.9579 (I)	...	...
5	$\omega_z = 120°/\mathrm{s}$	3.0096 (I)	...	...
6	$\dot{\omega}_z = 1°/\mathrm{s}^2$	3.1647 (I)	...	...
7	$\dot{\omega}_z = 2°/\mathrm{s}^2$	3.1148 (D)	...	...
Apple iPhone 5S Z-Gyro				
0	$\omega_z = 0°/\mathrm{s}$	1.034	1.7101, 7.049	9.7259e-3, 1.0601
1	$\omega_z = 9°/\mathrm{s}$	1.483 (I)	1.812, 10.9602 (I)	1.5432e-2, 0.9763 (I)
2	$\omega_z = 18°/\mathrm{s}$	2.6197 (I)	6.9739 (D), 17.709 (I)	7.2487e-2, 1.7943
3	$\omega_z = 36°/\mathrm{s}$	1.7224	1.8926 (D), 18.4464 (I)	1.4675e-2, 1.149188 (I)
4†	$\omega_z = 72°/\mathrm{s}$	...	...	...
5	$\omega_z = 120°/\mathrm{s}$	3.4084 (I)	0.16507 (D), 0.3293	1.6252e-2, 1.26445 (I)
6	$\dot{\omega}_z = 1°/\mathrm{s}^2$	2.3335 (I)	1.4157 (D), 24.854 (I)	...
7	$\dot{\omega}_z = 2°/\mathrm{s}^2$	1.6842 (D)	1.4488 (I), 23.8911 (D)	...

(I) Increased, (D) decreased, † contaminated dataset.

GM processes could be recognized. Table 4 shows how the values of σ^2_{GM1} and β_1 are hardly changed according to increasing $\dot{\omega}_z$ from 1 to 2 deg/s^2.

Based on the proposed contamination test results, the data set collected for Experiment 4 (where 72 deg/s angular velocity was applied to the Apple iPhone 5S Z-Gyro) is considered to include outliers. As a result, no analysis was performed for such data set in Table 4. Comparing values of WN parameter identified in Table 2 and Table 4, it is clear how both AV and GMWM can successfully detect the behaviour of WN variance according to different applied dynamics. However, an obvious shift of such variance value could be noticed. Therefore, the next step is to carry out a model verification approach in order to accurately determine which method is better.

4. TESTING AND VALIDATION USING PROPOSED DYNAMICALLY DEPENDENT ADAPTIVE INS/GPS NAVIGATION ALGORITHM

This section is dedicated for two main reasons:

1. Study the performance of the estimated model parameters based on both previously mentioned methods, AV and GMWM.

2. Introduce a dynamically dependent adaptive INS/GPS integrated navigation algorithm. Such an adaptive feature is related to the stochastic sensor error modeling.

In order to achieve that, simulation results are introduced in three steps. First, a deterministic calibration is performed to the smartphone's MEMS-based IMU. Inertial module for the Apple iPhone 5S was selected based on the results listed in Table 2 and Table 4, respectively. Where, in Table 2 the AV was used, the identified stochastic model structure for the Apple iPhone 5S gyro is, mostly, based on WN process. On the other hand, in Table 4 where the GMWM was used, the identified stochastic model structure for the same gyro is a combination of WN added to two 1st order GM processes. Such a difference in the model structure worth to be tested to check the accuracy of each structure individually. It is also important to mention that data sheet of the ST-Microelectronics, L3G4200DH gyros, mounted on the Apple iPhone 5S, provided by the manufacturer does not provide guaranteed information regarding the stochastic characteristics of such sensors. Such circumstance strongly emphasizes the importance of our stochastic analysis.

We adopted the six-position static calibration test to determine both the deterministic bias and scale factor of gyros and accelerometers. Briefly, the six-position test involves mounting the inertial instrument on a leveled surface with its axis pointing alternately up followed by down. For a triad of orthogonal sensors, this leads to a total six positions. For accelerometer and gyro, in order to determine their bias and scale factor, summing and differencing measurements is required, respectively. More detailed information and equations about such technique could be found in [2]. Based on the above, obtained biases and scale factors were being compensated through the following observation equations of both angular rates and specific forces for gyro and accelerometer, respectively [2].

$$\omega = \omega_{true} + b_\omega + S_\omega \omega + c_\omega t + \varepsilon_\omega, \quad (9)$$

$$f = f_{true} + b_f + S_f f + c_f t + \varepsilon_f, \quad (10)$$

where ω is the gyro output measurement, ω_{true} is the true rotation rate around the gyro sensitive axis, b_ω is the gyro bias, S_ω is the gyro scale factor, c_ω is the temperature coefficient of gyro family, t is the temperature, f is the accelerometer output measurement, f_{true} is the true specific force along the accelerometer longitudinal axis, b_f is the accelerometer bias, S_f accelerometer scale factor, c_f is the temperature coefficient of accelerometer family and $\varepsilon_{\omega,f}$ are the sensor noises. As mentioned in the Introduction section, temperature variation effect is neglected here in this paper due to the relatively short duration data sets. Consequently, c_ω and c_f values are considered to be zeros.

Thus, obtained values for biases and scale factors, for gyros and accelerometers, in additional to the stochastic specifications provided by the manufacturer for Bosch Sensortec BMA220 accelerometers were being used as inputs to IMU Simulator (IMUS) Toolbox, which is the second step of our simulation. The IMUS was developed by the Mobile Multi-Sensors System (MMSS) research group at the UofC and it has the ability to generate simulated inertial sensor measurements (i.e. accelerations and angular rotations) based on two inputs, IMU specifications and a designed trajectory. In other words, it provides the simulated data of any IMU grade. Moreover, such a tool can generate a variety of sensor errors such as constant bias, scale factor errors and random walk, using datasheet characteristics provided by the manufacturers or obtained through lab testing, and their combinations in any data rate specified by the user. Based on a variety of vehicle dynamics such as straight line, accelerations and turns, the simulator can design any trajectory for any application and, hence, provides GPS position and velocity simulated measurements, according to GPS parameters values defined by the user. Moreover, such an inverse INS mechanization tool has the ability to divide the pre-designed trajectory into successive segments, will be illustrated through Fig. 13, where utilized model parameters could be changed based on the user's criterion. Thus, the theoretical inertial sensor outputs that should be observed along the designed trajectory are obtained.

In our test, a multi turns trajectory was designed (Figure 13) for a moving vehicle in the horizontal

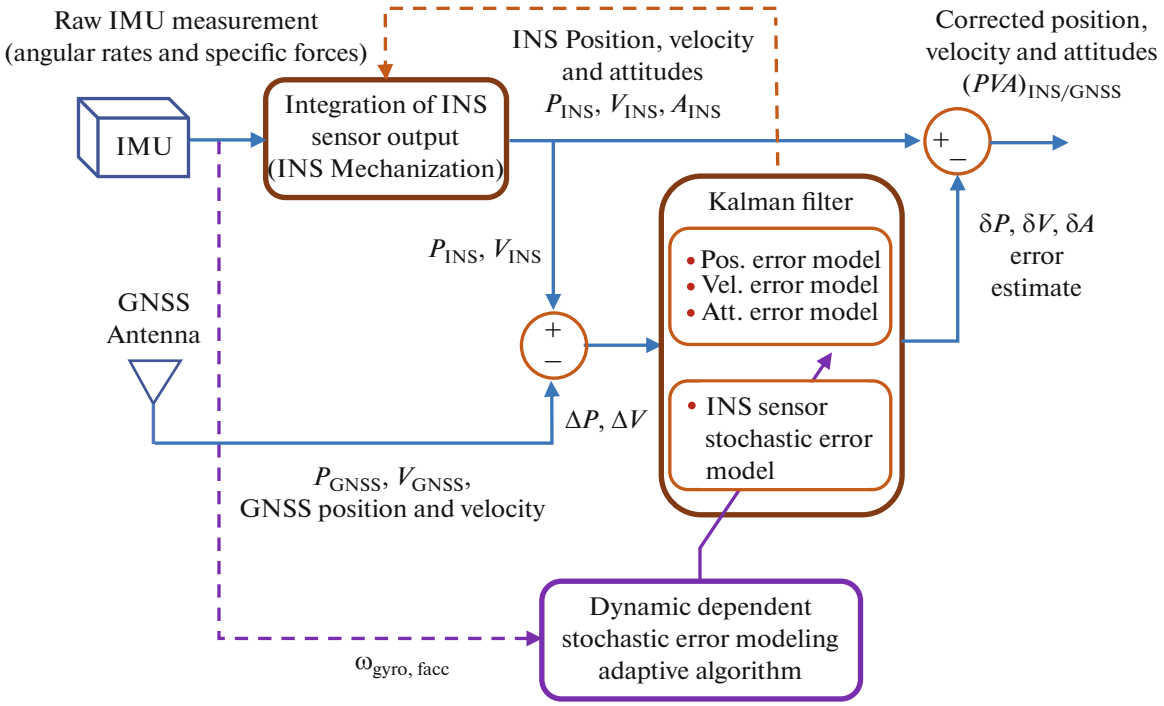

Fig. 12. INS mechanization and dynamically dependent error modeling in INS/GNSS integration for AINS+.

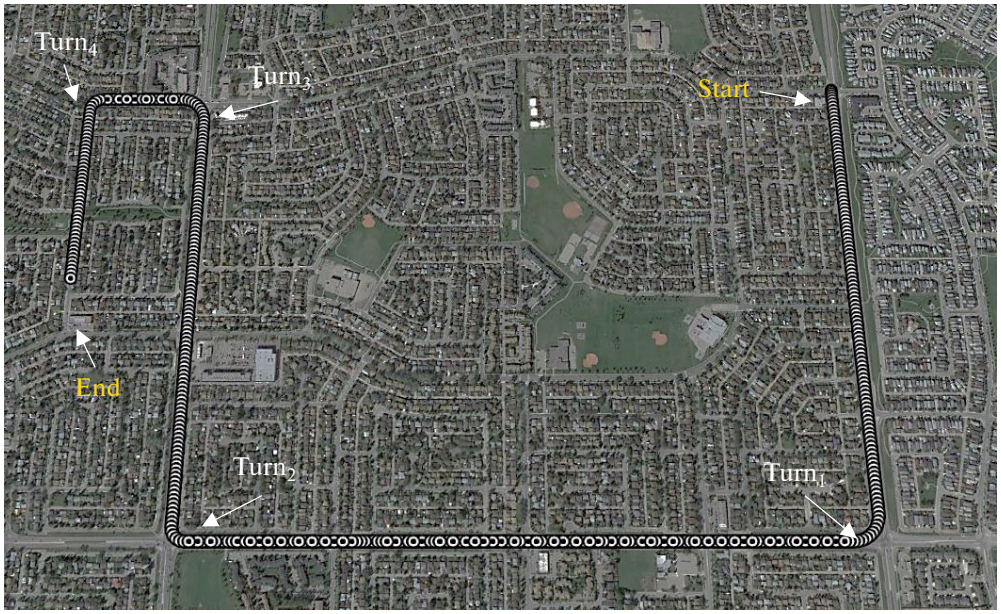

Fig. 13. Multi-turns designed trajectory of the simulation test.

plane. IMUS provides two output files, raw IMU data and reference trajectory data. Both files are being fed as inputs to the new proposed dynamically dependent loosely coupled-based Aided Inertial Navigation System (AINS+) Toolbox, which is an extended modified version of the Aided Inertial Navigation System Toolbox (AINS) of UofC introduced by [31], as a third step of our simulation.

In our simulation, the external aiding integrated with inertial data are represented as the reference INS/GPS-based data trajectory generated as illustrated in the second step. However, for the standard AINS algorithm, sensor errors are described using 1st order GM models and their related parameters can be set "once" as a priori information. In other words, fixed values for the stochastic model parameters are

fed to the used algorithm with no ability to change these values under any environmental conditions during the algorithm operation. In the Experiments and Results section, we showed that such model parameters are not fixed and could vary according to the platform dynamics. Such variation could directly affect the accuracy of the integrated INS/GPS system. This implies that using a fixed error model in filter design for the standard AINS algorithm is a major drawback, especially for a changing dynamics environment. Based on this point of view, the fixed stochastic error model approach should be replaced by an adaptive dynamically dependent one.

In this section, we introduce a dynamically dependent extension for the AINS algorithm, namely AINS+. Such a modified algorithm gives the user better opportunity to feed more than a single value for each stochastic error parameters, according to the applied angular velocity, through an additional adaptive function and in the sense of multi-model based estimation.

Moreover, the innovation part of the AINS+ refers to adding a separate feedback, as shown in Fig. 12 which is a general layout of the proposed adaptive algorithm, from the raw sensor output which is being used as follow:

(1) Check the sensor output measurements, for instance the gyro output angular rate, and feed them to the dynamic dependent stochastic error modeling adaptive algorithm which, in turn, detect the dynamic level applied on the platform. More details about evaluated models will be discussed through the validation procedure sequence.

(2) Based on Step 1, a stochastic model parameters values selection criterion is being used to selects the appropriate model values and use them through the INS sensor stochastic error model part.

The designed trajectory, illustrated in Fig. 13, contains straight lines and turns with about 8 minutes total kinematic period. Turns were carefully designed to represent different applied angular velocity to the vertical axis as follow:

■ $\omega_z = 9^\circ/\text{s}$ for 10 s at $Turn_1$ and $Turn_3$, Clock Wise (CW) and Counter Clock Wise (CCW) respectively. Thus, a 90° turns are applied.

■ $\omega_z = 18^\circ/\text{s}$ for 5s at $Turn_2$ and $Turn_4$, CW and CCW respectively. Thus, a 90° turns are applied.

The main reason for including multiple turns with different applied angular velocities is to compare the performance of pre-estimated stochastic models based on static, AV and GMWM approaches during each turn.

Consequently, validation procedure sequence used in this section could be highlighted as follow:

• A precise full INS/GPS navigation solution for the aforementioned trajectory is computed using AINS+ toolbox and considered as a reference trajectory.

• The real stochastic error parameters acquired by the IMU under test, Apple iPhone 5S IMU, are added to the inertial signals simulated by IMUS toolbox.

• Relatively short artificial GPS signal outages, 10s each (very common to occur in practice) were introduced. Such GPS signal outages cover the four previously mentioned 90° turns.

• The quality of three different stochastic models is judged by comparing their corresponding trajectories' position errors at the end of each GPS signal outage period compared to the reference trajectory.

The three gyro stochastic models to be validated are defined as:

■ M_{static} = WN based on AV analysis for static data as shown in Table 1 (dynamic dependency feature is disabled here to evaluate model parameters obtained from static data).

■ $M_{\text{dynamic(AV)}}$ = WN based on AV analysis for dynamics data as shown in Table 2, Exp.1 for Apple iPhone 5S (dynamic dependency feature is enabled here).

■ $M_{\text{dynamic(GMWM)}}$ = WN + 2GM based on GMWM analysis for dynamics data as shown in Table 4, Exp.1 for Apple iPhone 5S (dynamic dependency feature is enabled here). As show in Table 4, the correlation time of the second 1st order GM process is quite high for our short-simulated trajectory. Consequently, the later model could be simplified as $M_{\text{dynamic(GMWM)}}$ = WN + GM.

• The proposed dynamically dependent part selects the appropriate model parameters values, for gyros, based on a feedback from the raw angular rate measured by the gyro (feedback line is highlighted with purple dashed line in Fig. 12). According to the aforementioned designed trajectory, selection criterion is highlighted in Table 5.

It is important to mention that such selection criterion, highlighted in Table 5, is based on the absolute value of the gyro output measurements to coop with both directions of rotations, CW and CCW.

Every sub-plot of Figure 14, which is a zoom-in for the four 90° turns of Figure 13, shows a comparison between: reference trajectory (green line) from the INS/GPS solution with no GPS outage, the KF with feedback solution implemented by AV-based static model (black line) with 10s GPS outage "M_{static}", the KF with feedback solution implemented by AV-based dynamic model (red line) with 10 s GPS outage "$M_{\text{dynamic(AV)}}$" and the KF with feedback solution implemented by GMWM-based dynamic model (blue line) with 10s GPS outage "$M_{\text{dynamic(GMWM)}}$".

Now, for each GPS signal outage we have three trajectories, each trajectory is based on a specific sto-

Table 5. Selection criterion for the dynamically dependent stochastic error modeling adaptive algorithm

Gyro output °/s	Stochastic model parameters values for Apple iPhone 5S Gyro	
	AV *Gyro Model = WN*	GMWM *Gyro Model = WN + GM*
|0–5|	Table 1. Exp. No. 0	Table 4. Exp. No. 0
|5–15|	Table 2. Exp. No. 1	Table 4. Exp. No. 1
|15–25|	Table 2. Exp. No. 2	Table 4. Exp. No. 2
|25–55|	Table 2. Exp. No. 3	Table 4. Exp. No. 3

chastic model. Thus, the position errors are computed by subtracting the INS/GPS solution that contains the GPS signal outage, at the end of the outage, from the reference solution. Then, the magnitude of the 2D position errors during the selected GPS outage was computed for each trajectory, individually. As shown in Fig. 14, the values of all position errors at the end of the outage period are represented by the dotted lines. For instance and regarding Fig. 14 (a), it is clear how the length of blue line, related to the trajectory based on the GMWM dynamic model, is the shortest line which indicates that such a model reflects better results than the other two models. Numerically, Table 6 clarify the effect of using a low-cost MEMS-based smartphone mounted IMU which is obvious in terms of the 2D position drift error values during the GPS

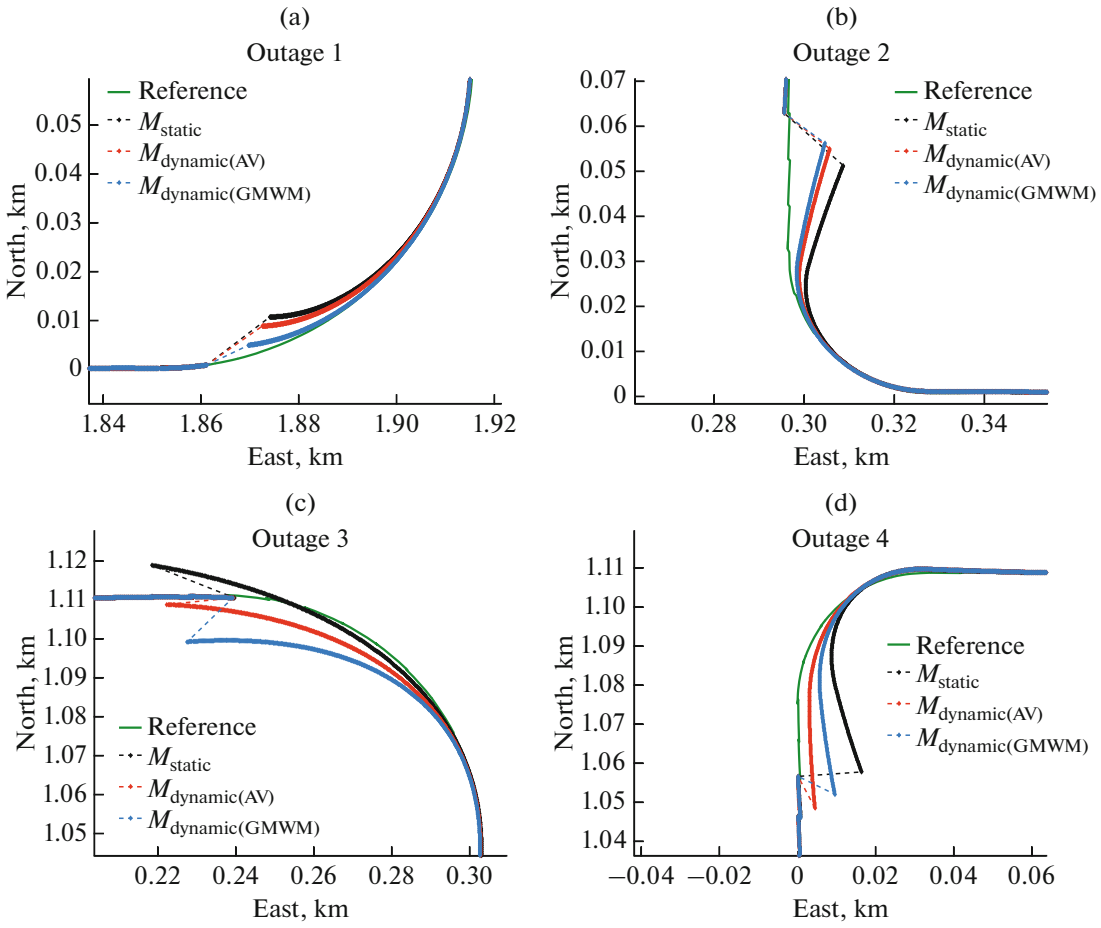

Fig. 14. Influence of different inertial sensor stochastic error models on estimated trajectory (black trajectory was introduced using a dynamically independent integrated navigation algorithm, AINS. Both red and blue trajectories was introduced using the new proposed dynamically dependent integrated navigation algorithm, AINS+).

Table 6. Position error during GPS signal outage using static, dynamic AV-based and dynamic GMWM-based models for modelling Apple iPhone 5S sensor errors

Model	2D Position drift after GPS signal outages (m)				
	outage 1 ($Turn_1$)	outage 2 ($Turn_2$)	outage 3 ($Turn_3$)	outage 4 ($Turn_4$)	mean
M_{static}	16.302	17.504	20.21	15.316	17.333
$M_{\text{dynamic(AV)}}$	14.401	12.822	16.101	**9.104**	13.107
$M_{\text{dynamic(GMWM)}}$	**9.866**	**11.214**	**11.761**	10.681	**10.881**

outage periods. Moreover, last column of Table 6 highlights the mean value of 2D position error related to each model. It is also worth to mention that the standard deviation values of the estimated states obtained from the KF covariance matrix (P-matrix) are matching the actual RMS errors obtained from the comparison of the reference solution with the estimated one.

It can be seen that results of Table 6 demonstrate the efficiency of GMWM model based on the dynamic analysis, $M_{\text{dynamic(GMWM)}}$, over other models. Significantly, GMWM-based dynamic model limits the overall error growth during the GPS signal outage periods more than the other two models.

In addition to the above and compared to the position error value induced by using M_{static}, the total position drift error (mean value) was improved by 24 and 37% when using $M_{\text{dynamic(AV)}}$ and $M_{\text{dynamic(GMWM)}}$, respectively. Moreover, such an improvement is reflected on the quality of the proposed dynamically dependent integrated navigation algorithm, AINS+, which is proven to be adaptive, form the stochastic modeling perspective, based on the applied platform dynamics.

Based on the previous analysis, it is clear that assuming random inertial error processes are to be independent of the dynamics of the platform on which the inertial sensors are mounted is not a precise assumption anymore. Consequently, performing a dynamic dependent error analysis associated with a dynamically adaptive integrated navigation algorithm is essential to minimize position error during GPS free periods. Moreover, GMWM approach is proven to be more accurate than the traditional AV one. The reason for that refers to the ability of GMWM to precisely detect correlated noise as a latent stochastic process in the gyro measurement. Such a correlated noise, represented in the form of multiple 1st order GM, included in the GMWM-based model structure which finally leaded to less position error compared to the AV-based and static-based models.

5. SUMMARY AND CONCLUSIONS

The dynamic dependent sensor stochastic error model for low-cost MEMS IMUs was investigated and analysed in this paper. Two different tools, namely the Allan Variance (AV) and the Generalized Method of Wavelet Moments (GMWM), were utilized for noise characterization related to inertial sensors residual measurements. The detailed estimation results were highlighted for both static and dynamic data sets collected at different applied dynamic quantities (angular velocity and acceleration) using two MEMS-based IMUs, InvenSense MPU-6500 and ST-Microelectronics L3G4200DH, mounted on two different smartphones, the Samsung Galaxy S4 and the Apple iPhone 5S, respectively. The AV/GMWM characteristic curves were constructed and used to identify the type and level of stochastic noise parameters in the output datasets for gyros of both MEMS IMUs. The same analyses were repeated for different applied dynamics that allowed identifying the general behavior of such parameters as a reflection of the platform dynamics variation.

Comparing the AV and GMWM methods showed that the classical AV could efficiently detect Angular Random Walks (ARWs) as well as their general pattern in both static and dynamic modes. As a demerit, the AV tool did not have the ability to detect any outliers in the data under test which could possibly lead to inaccurate modeling for the measured signals. On the other hand, the recently proposed GMWM overcame this problem by comparing the classical WV with another robust one using the so-called robust (or contamination) test. Moreover, the GMWM could successfully identify correlated noise parameters represented in the sum of one or more 1st order Gauss-Markov (GM) processes which never could be discriminated using the AV. The main reason for that was revealed to be related to the slope fitting analysis technique utilized through the AV approach. Such a technique degraded the accuracy of the AV regarding correlated noise processes identification.

Moreover, different candidate models were evaluated by the proposed Wavelet Information Criteria

(WIC) that compromise the goodness-of-fit of each model and its related complexity, which is considered an additional merit of the GMWM over the AV. The model selection results indicated that the noise model structure was not affected by the applied dynamics. Only model parameters' values differ according to dynamic variations. Consequently, augmented stochastic noise models in a navigation Kalman Filter (KF) will have the same structure but with different parameter magnitudes depending on the applied dynamics.

The validity of pre-estimated models was verified by augmenting means of simulated specific forces and angular rates corrupted by the real error signals, for the Apple iPhone 5S IMU, into a new dynamically dependent integrated navigation algorithm, namely AINS+. Such an algorithm uses an additional selection criterion to switch between different stochastic error parameters values according to the applied platform dynamics. This enabled eliminating dynamics-dependent effects. The related stochastic error model was compensated via different configurations based on static, dynamic AV-based and dynamic GMWM-based analysis. These configurations were compared to a full INS/GPS navigation solution and their performances were investigated during GPS signal outage periods. The results showed that for the inertial standalone performance during GPS signal outages, the obtained position accuracy is improved when using dynamic dependent stochastic error models, associated with the new proposed dynamically adaptive algorithm, instead of the commonly used non-adaptive static one. Moreover, it has been demonstrated that the GMWM-based stochastic model outperforms the AV-based one in terms of a 2D position drift at the end of the GPS signal free periods. As recommendations, we need to use more complicated stochastic models rather than the traditional AV-based ones with taking into consideration the correct choice of different parameter setting according to platform dynamic variations which, in turn, requires a dynamically dependent adaptive integrated navigation algorithm. Such recommendations could strongly improve the overall performance for low-cost INS/GNSS integrated navigation system.

To further promote this approach, other high-end IMUs should be investigated and more error models should be designed which will be investigated in our future work.

Acknowledgments: The data used in this paper was collected in the PLAN Group Lab at the University of Calgary. We would like to thank Dr. Thyagaraja Marathe, Postdoctoral Fellow, Department of Geomatics Engineering at the University of Calgary for his help in operating the Animatics SmartMotor™ Series 4 Single Axis Positioning and Rate Table.

Author Contributions: A.R. designed and performed the experiments, analyzed the data, wrote the paper. N.E. provided the general direction on the methodology of the paper. S.N. and N.E. reviewed and revised the paper.

Conflicts of Interest: The authors declare no conflict of interest.

REFERENCES

1. A. B. Jensen, "*GNSS Satellite Orbits*," *Technical University of Denmark,* 2010.
2. N. El-Sheimy, "Lecture note 623—Inertial Techniques and INS/DGPS Integration," ed: Department of Geomatics Engineering, University of Calgary, 2014.
3. S. Nassar, Z. Syed, X. Niu, and N. El-Sheimy, "Improving MEMS IMU/GPS systems for accurate land-based navigation applications," in *ION NTM*, 2006, pp. 523–529.
4. O. J. Woodman, "An introduction to inertial navigation," *University of Cambridge, Computer Laboratory, Tech. Rep. UCAMCL-TR-696,* vol. 14, p. 15, 2007.
5. X. Niu, S. Nasser, C. Goodall, and N. El-Sheimy, "A universal approach for processing any MEMS inertial sensor configuration for land-vehicle navigation," *The Journal of Navigation,* vol. 60, no. 2, pp. 233–245, 2007.
6. S. Nassar, *Improving the inertial navigation system (INS) error model for INS and INS/DGPS applications*. National Library of Canada= Bibliothèque nationale du Canada, 2005.
7. Y. Li, J. Georgy, X. Niu, Q. Li, and N. El-Sheimy, "Autonomous calibration of MEMS gyros in consumer portable devices," *IEEE Sensors Journal,* vol. 15, no. 7, pp. 4062–4072, 2015.
8. X. Niu, Z. Gao, R. Zhang, Z. Chen, and J. Dong, "Micro-machined attitude measurement unit with application in satellite TV antenna stabilization," in *Symposium Gyro Technology 2002, Stuttgart, Germany*, 2002, p. 2002.
9. Y. Li, H. Lan, Y. Zhuang, P. Zhang, X. Niu, and N. El-Sheimy, "Real-time attitude tracking of mobile devices," in *Indoor Positioning and Indoor Navigation (IPIN), 2015 International Conference on*, 2015, pp. 1–7: IEEE.
10. N. El-Sheimy, H. Hou, and X. Niu, "Analysis and modeling of inertial sensors using Allan variance," *IEEE Transactions on instrumentation and measurement,* vol. 57, no. 1, pp. 140–149, 2008.
11. J. R. Evans *et al.*, "Method for calculating self-noise spectra and operating ranges for seismographic inertial sensors and recorders," *Seismological research letters,* vol. 81, no. 4, pp. 640–646, 2010.
12. P. Petkov and T. Slavov, "Stochastic modeling of MEMS inertial sensors," *Cybernetics and information technologies,* vol. 10, no. 2, pp. 31–40, 2010.
13. D. Magill, "Optimal adaptive estimation of sampled stochastic processes," *IEEE Transactions on Automatic Control,* vol. 10, no. 4, pp. 434–439, 1965.
14. S. Dmitriev, D. Koshaev, and O. Stepanov, "Multichannel filtration and its application in removing ambi-

guity when positioning objects by using the GPS," *Journal of Computer and Systems Sciences International,* vol. 36, no. 1, pp. 57–62, 1997.

15. X. R. Li and V. P. Jilkov, "Survey of maneuvering target tracking. Part V. Multiple-model methods," *IEEE Transactions on Aerospace and Electronic Systems,* vol. 41, no. 4, pp. 1255–1321, 2005.
16. D. W. Allan, "Statistics of atomic frequency standards," *Proceedings of the IEEE,* vol. 54, no. 2, pp. 221–230, 1966.
17. X. Zhang, Y. Li, P. Mumford, and C. Rizos, "Allan variance analysis on error characters of MEMS inertial sensors for an FPGA-based GPS/INS system," in *Proceedings of the International Symposium on GPS/GNNS*, 2008, pp. 127–133.
18. M. Marinov and Z. Petrov, "Allan variance analysis on error characters of low-cost MEMS accelerometer MMA8451Q," in *International conference of scientific paper AFASES*, 2014.
19. J. Li and J. Fang, "Not fully overlapping Allan variance and total variance for inertial sensor stochastic error analysis," *IEEE Transactions on Instrumentation and Measurement,* vol. 62, no. 10, pp. 2659–2672, 2013.
20. A. Hussen and I. Jleta, "Low Cost Inertial Sensors Modeling Using Allan Variance," *World Academy of Science, Engineering and Technology, International Journal of Computer, Electrical, Automation, Control and Information Engineering,* vol. 9, no. 5, pp. 1237–1242, 2015.
21. S. Guerrier, J. Skaloud, Y. Stebler, and M.-P. Victoria-Feser, "Wavelet-variance-based estimation for composite stochastic processes," *Journal of the American Statistical Association,* vol. 108, no. 503, pp. 1021–1030, 2013.
22. J. Balamuta, R. Molinari, S. Guerrier, and W. Yang, "The gmwm R package: a comprehensive tool for time series analysis from state-space models to robustness," *arXiv preprint arXiv:1607.04543,* 2016.
23. J. Balamuta, S. Guerrier, R. Molinari, and W. Yang, "A Computationally Efficient Framework for Automatic Inertial Sensor Calibration," *arXiv preprint arXiv:1603.05297,* 2016.
24. S. Guerrier, R. Molinari, and Y. Stebler, "Wavelet-Based Improvements for Inertial Sensor Error Modeling," *IEEE Transactions on Instrumentation and Measurement,* vol. 65, no. 12, pp. 2693–2700, 2016.
25. Y. Yuksel, N. El-Sheimy, and A. Noureldin, "Error modeling and characterization of environmental effects for low cost inertial MEMS units," in *Position Location and Navigation Symposium (PLANS), 2010 IEEE/ION*, 2010, pp. 598–612: IEEE.
26. P. Aggarwal, Z. Syed, X. Niu, and N. El-Sheimy, "Cost-effective testing and calibration of low cost MEMS sensors for integrated positioning, navigation and mapping systems," in *Proceedings of XXIII FIG Congress, Munich, Germany*, 2006, vol. 813.
27. M. El-Diasty, A. El-Rabbany, and S. Pagiatakis, "Temperature variation effects on stochastic characteristics for low-cost MEMS-based inertial sensor error," *Measurement Science and Technology,* vol. 18, no. 11, p. 3321, 2007.
28. M. Wis and I. Colomina, "Dynamic dependency of inertial sensor errors and its application to INS/GNSS navigation," *Proc. NAVITEC Congr,* pp. 1–7, 2010.
29. Y. Stebler, S. Guerrier, J. Skaloud, R. Molinari, and M.-P. Victoria-Feser, "Study of MEMS-based inertial sensors operating in dynamic conditions," in *2014 IEEE/ION Position, Location and Navigation Symposium-PLANS 2014*, 2014, pp. 1227–1231: IEEE.
30. A. Radi, N. Elsheimy, and Y. Li, "Temperature Variation effects on the Stochastic Performance of Smartphone Sensors Using Allan Variance and Generalized Method of Wavelet Moments," ed. *Proceedings of the 2017 International Technical Meeting of The Institute of Navigation, Monterey, California, January 2017*, pp. 1242–1255, 2017.
31. E. Shin and N. El-Sheimy, "Aided Inertial Navigation System (AINS™) Toolbox for MatLab® Software," *INS/GPS integration software, Mobile Multi-Sensors System (MMSS) research group, the University of Calgary* http://mms. *geomatics. ucalgary. ca/Research/Tech% 20transfer/INS_toolbox. htm,* 2004.
32. A. G. Hayal, "*Static calibration of the tactical grade inertial measurement units*," The Ohio State University, 2010.
33. P. G. Savage, "Analytical modeling of sensor quantization in strapdown inertial navigation error equations," *Journal of Guidance, Control, and Dynamics,* vol. 25, no. 5, pp. 833–842, 2002.
34. I. o. E. a. E. Engineers, *IEEE Standard Specification Format Guide and Test Procedure for Linear, Single-axis, Nongyroscopic Accelerometers.* IEEE, 1999.
35. W. Abdel-Hamid, *Accuracy enhancement of integrated MEMS-IMU/GPS systems for land vehicular navigation applications*. Library and Archives Canada= Bibliothèque et Archives Canada, 2006.
36. S. Guerrier, R. Molinari, and Y. Stebler, "Theoretical Limitations of Allan Variance-based Regression for Time Series Model Estimation," *IEEE Signal Processing Letters,* vol. 23, no. 5, pp. 597–601, 2016.
37. X. Niu *et al.*, "Using Allan variance to analyze the error characteristics of GNSS positioning," *GPS solutions,* vol. 18, no. 2, pp. 231–242, 2014.
38. H. Hou, *Modeling inertial sensors errors using Allan variance*. Library and Archives Canada= Bibliothèque et Archives Canada, 2005.
39. R. J. Vaccaro and A. S. Zaki, "Statistical modeling of rate gyros," *IEEE Transactions on Instrumentation and Measurement,* vol. 61, no. 3, pp. 673–684, 2012.
40. D. B. Percival and P. Guttorp, "Long-memory processes, the Allan variance and wavelets," *Wavelets in geophysics,* vol. 4, pp. 325–344, 1994.
41. D. B. Percival and A. T. Walden, *Wavelet methods for time series analysis.* Cambridge university press, 2006.
42. Y. Stebler, S. Guerrier, J. Skaloud, and M.-P. Victoria-Feser, "A framework for inertial sensor calibration using complex stochastic error models," in *Position*

Location and Navigation Symposium (PLANS), 2012 IEEE/ION, 2012, pp. 849–861: Ieee.

43. S. Guerrier and R. Molinari, "Wavelet variance for random fields: an m-estimation framework," *arXiv preprint arXiv:1607.05858,* 2016.
44. S. Guerrier, R. Molinari, and J. Skaloud, "Automatic identification and calibration of stochastic parameters in inertial sensors," *Navigation,* vol. 62, no. 4, pp. 265–272, 2015.
45. Y. Stebler, S. Guerrier, J. Skaloud, and M.-P. Victoria-Feser, "Generalized method of wavelet moments for inertial navigation filter design," *IEEE Transactions on Aerospace and Electronic Systems,* vol. 50, no. 3, pp. 2269–2283, 2014.
46. A. IFIXIT, "Apple iPhone 5s."
47. T. R. Kane and D. A. Levinson, *Dynamics, theory and applications.* McGraw Hill, 1985.
48. W. Ding, J. Wang, Y. Li, P. Mumford, and C. Rizos, "Time synchronization error and calibration in integrated GPS/INS systems," *ETRI journal,* vol. 30, no. 1, pp. 59–67, 2008.
49. Y. Stebler, S. Guerrier, and J. Skaloud, "An approach for observing and modeling errors in MEMS-based inertial sensors under vehicle dynamic," *IEEE Transactions on Instrumentation and Measurement,* vol. 64, no. 11, pp. 2926–2936, 2015.